Full Length Article

Assessing changes in mangrove forest cover and carbon stocks in the Lower Mekong Region using Google Earth Engine

Megha Bajaj [a], Nophea Sasaki [a,*], Takuji W. Tsusaka [a], Manjunatha Venkatappa [a,b], Issei Abe [c], Rajendra P. Shrestha [a]

[a] Natural Resources Management, Department of Development and Sustainability, Asian Institute of Technology, Pathum Thani, 12120, Thailand
[b] LEET Intelligence Co., Ltd., Suan Prikthai, Muang Pathum Thani, Pathum Thani, 12000, Thailand
[c] Kyoto Koka Wowen University, Kyoto, Japan

A B S T R A C T

The Lower Mekong Region (LMR) faces significant loss of mangrove forests, yet limited studies have explored this decline in the region. Here, we employ Google Earth Engine and Landsat satellite imagery to assess changes in mangrove forest cover across Myanmar, Thailand, Vietnam, and Cambodia between 1989 and 2020, with a five-year interval. Accordingly, we estimated carbon stock changes due to changes of forest cover. Our analysis yielded an overall average accuracy of 92.10% and an average kappa coefficient of 0.89 across the four countries. The findings reveal a 0.9% increase in mangrove area in Myanmar, 2.5% in Thailand, and 1.3% in Cambodia, while Vietnam experienced a 0.2% loss annually between 1989 and 2020. Carbon stocks in mangrove forests were estimated at 577.0 Tg of carbon or TgC, 250.0 TgC, 61.6 TgC, and 269.0 TgC in 1989 for Myanmar, Thailand, Cambodia, and Vietnam respectively, and increased to 736.0 TgC, 443.0 TgC, 86.7 TgC, and 254 TgC in 2020. Increase in mangrove areas resulted in carbon removals of 42.8 $TgCO_2$ $year^{-1}$ over the same period above. Depending on policies in these respective countries, such carbon removals could be used to claim for result-based payment under the REDD + scheme of the United Nations Framework Convention on Climate Change.

1. Introduction

Spanning latitudes of 25–30°N and 25–30°S (FAO, 2020) and characterized by their unique ability to thrive in subtropical coastal regions, mangroves are vital ecosystems supporting local and national development (Saxena & Jain, 2017; Sathe et al., 2013). Globally, mangrove forest cover has experienced a rapid decline from 18.8 million hectares (Mha) in 1980 (FAO, 2007) to 13.7 Mha in 2000 (Chen et al., 2017). Despite a slight recovery to 15.5 Mha in 2005 (FAO, 2007), the overall trajectory continued to trend downwards, reaching 14.8 Mha in 2020 (FAO, 2020). The net decrease was 1.04 Mha between 1990 and 2020 (FAO, 2020) (Figs. SI–1). Most mangroves are founded in Asia, covering 5.55 Mha (FAO, 2020) or approximately 39% of the total global mangrove area (Jia et al., 2023; Thomas et al., 2017). Changes of mangrove cover in the Lower Mekong Region (LMR), which includes Myanmar, Thailand, Vietnam, and Cambodia have been influenced by geopolitical shifts and growing demands in the region but such changes have not been assessed in the LMR, hindering the introduction of appropriate measures to prevent further losses and facilitate restoration and conservation efforts (Asner et al., 2010).

Assessing changes in mangrove cover serves as a baseline for restoration targets (Lovelock et al., 2022), making it possible for regular monitoring that can lead to reduction of mangrove loss (Kanniah et al., 2015). Such assessment became possible recently through the applications of the Google Earth Engine (GEE) as the GEE has emerged as a powerful and versatile tool with a wide range of monitoring applications in various environmental fields. For example, the GEE has been utilized to address pressing environmental challenges and provide data-driven insights in the monitoring of land cover changes (Song et al., 2018), assessing deforestation rates (Hansen et al., 2013), tracking urban growth (Li et al., 2021), mapping wildfire dynamics (Cohen et al., 2017), and even predicting disease outbreaks (Funk et al., 2018). Furthermore, GEE's cloud-based infrastructure offers significant computational power, enabling the analysis of vast datasets (Dandois and Ellis, 2013) and facilitating timely decision-making in response to environmental changes (Lechner et al., 2018). Amid this wealth of applications, GEE's role in

assessing mangrove forest cover changes is of paramount importance. Its capacity to process and analyze satellite imagery over extended time-frames (Xiong et al., 2017) makes it a valuable tool for studying dynamic ecosystems like mangrove forests. In fact, GEE has been successfully employed to monitor mangrove deforestation and restoration in regions such as the Sundarbans in Bangladesh and India (Saha et al., 2020) and the Caribbean (Caldwell et al., 2019). In addition, GEE facilitates the integration of data from multiple sources, including remote sensing and geographic information systems, enabling comprehensive assessments of mangrove ecosystems (Fuchs et al., 2020).

Utilizing the applications of the GEE, our study aims at assessing the changes in mangrove forest cover and carbon stocks in the LMR delineating by longitudes 92.2°E to 109°E and latitudes 21.5°N to 5.57°N. The LMR territories are intersected by the 4900 km of the Mekong River, culminating in a significant delta before reaching the ocean. The changes of mangrove forest cover were assessed between 1989 and 2020. Subsequently, the related carbon emissions and sequestration are also assessed to establish a forest reference emission level or FREL for the whole LMR. This FREL serves as a benchmark for assessing changes in carbon emissions resulting from the implementation of activities of Reducing Emissions from Deforestation and Forest Degradation, plus the conservation of forest, sustainable management of forests, and enhancement of forest carbon stocks (REDD+) in LMR.

Our research fills a scientific gap by providing a comprehensive, data-driven analysis of mangrove cover changes over three decades in the LMR between 1989 and 2020. Our study offers a novel approach in employing GEE for mangrove forest cover monitoring, setting a new benchmark in the field. The study findings can contribute to our understanding of the current state of mangrove cover, which is invaluable for aiding better-informed decision making in the conservation and restoration of mangrove forests. These important contributions are in line with multiple Sustainable Development Goals (SDGs) namely, SDG 6 (clean water), 12 (responsible consumption and production), 13 (climate action) and SDG 14 and 15 (life below water and life on land) (Bimrah et al., 2022; United Nations, 2022; Sasmito et al., 2023). The mangrove ecosystem restoration is also aligned with various international and national commitments and initiatives such as the Bonn Challenge, the New York Declaration on Forests, the United Nations Decade on Ecosystem Restoration, and national restoration targets specified in nationally determined contributions. In addition, our study could contribute to the implementation of the United Nations Convention to Combat Desertification (UNCCD)'s tenure-restoration targets for land degradation neutrality (UNCCD, 2014), which were adoption by more than 130 countries to halt, and then reverse the future land degradation (UNCCD, 2022). Such global initiatives underscore a widespread commitment to rejuvenate degraded mangrove ecosystems (FAO, 2023).

2. Literature review

Although the Asian continent is home to approximately 38% of the global mangrove forests (Thomas et al., 2017), the mangrove forests in Southeast Asia are diminishing rapidly, with annual loss rates between 3.6% and 8.1% (Hamilton & Casey, 2016). Such loss has particularly occurred in the LMR. For example, political instability and population growth have contributed to environmental and economic damage in Myanmar (Wang et al., 2013). In Cambodia, intensive logging occurred in the late 1980s during the nation's transition from a socialist state to a market economy, while Thailand's dependence on Cambodia's forests, including mangroves increased following its logging ban in 1989 (Le Billon, 2000). Vietnam also experienced a transition to a more market-oriented economic system in 1989, leading to unsustainable shrimp farming practices in the early 1990s that negatively impacted mangrove forests (De Graaf & Xuan, 1998). Mangrove ecosystems, renowned for their ability to sequester carbon, were estimated to store around 937 MgCO$_2$ (1 Megagram CO$_2$ = 1 ton of carbon dioxide) per hectare (Alongi, 2014). However, the alarming rates of mangrove loss,

primarily attributed to human activities and, to some extent, natural disasters (Sathe et al., 2013; Chakravarty et al., 2012; Malik et al., 2017), have significant environmental consequences. This loss leads to substantial carbon emissions, with Hamilton et al. (2016) estimating emissions of approximately 70–420 TgCO$_2$ (Teragrams of carbon dioxide = 1 million tons of carbon dioxide) annually between 2000 and 2012 due to mangrove deforestation. Therefore, understanding the changes in mangrove cover during these critical periods is essential for enhancing their protection.

The GEE, in conjunction with Google Cloud, provides a powerful platform for data accumulation and storage in Google Cloud Storage. A notable data repository in GEE is the Landsat satellite imagery collection, which supplies earth surface snapshots with approximately 30 m resolution every fortnight (Landsat Collections in Earth Engine Data Catalog, 2021). The GEE has been increasingly used for mangrove forest and other environmental monitoring. The innovative platform facilitates the analysis of long-term environmental changes, influenced by both anthropogenic and natural factors (Xie et al., 2019; Jia et al., 2021; Upakankaew et al., 2022). With its high-resolution satellite imagery and advanced computing capabilities, GEE offers a comprehensive approach for mapping and understanding mangrove forest dynamics (Jia et al., 2021). Utilized GEE and multi-temporal Landsat data a recent study was conducted to map and monitor mangrove forests in the Sundarbans Reserved Forest, Bangladesh with high overall accuracy of 90.3% (Rahman & Deddy, 2021). Another study in the Niger Delta, Nigeria, highlighted GEE's potential for mapping coastal land cover change, including mangrove forests, with high accuracy (89.2%) using time series Landsat data (Ibe et al., 2022). The findings in the studies showcase GEE's capabilities in providing robust, accurate, and scalable solutions for mangrove forest monitoring, especially in the Lower Mekong Region.

3. Study methodology

3.1. Data collection

In this study, we exploited the capabilities of Landsat 5 Thematic Mapper ™ and Landsat 8 Operational Land Imager (OLI) Tier 1 Top of Reflectance (TOA) imagery, accessible within GEE (Venkatappa et al., 2019). Due to data unavailability affected by changes of remote sensing technologies, we used the Landsat 5 to analyze mangrove forests for the years 1989, 1995, 2000, 2005, and 2010, while Landsat 8 was employed for 2015 and 2020 (Table 1) along the inclusive of coastal areas extending 5 km inland from the coastline of the LMR (Fig. 1). This is because mangrove forests predominantly occur within a 5 km radius from the coastline (Giri et al., 2011). We delineated a 5 km inland polygon in the LMR coastline using ArcMap 10.3.1. This delineated polygon was then imported to the GEE platform through the GEE asset manager, paving the way for in-depth analysis concentrating on the LMR coastal areas and the encompassed mangrove forest cover.

3.2. Data preprocessing and processing in Google Earth Engine

Data analysis was carried out through the JavaScript API on the GEE platform. The platform features a web-based Integrated Development Environment (IDE), dubbed the Code Editor, which facilitates the

Table 1
Image collections from landsat 5 and landsat 8 on Google Earth Engine for mangrove cover estimation in the Lower Mekong Region.

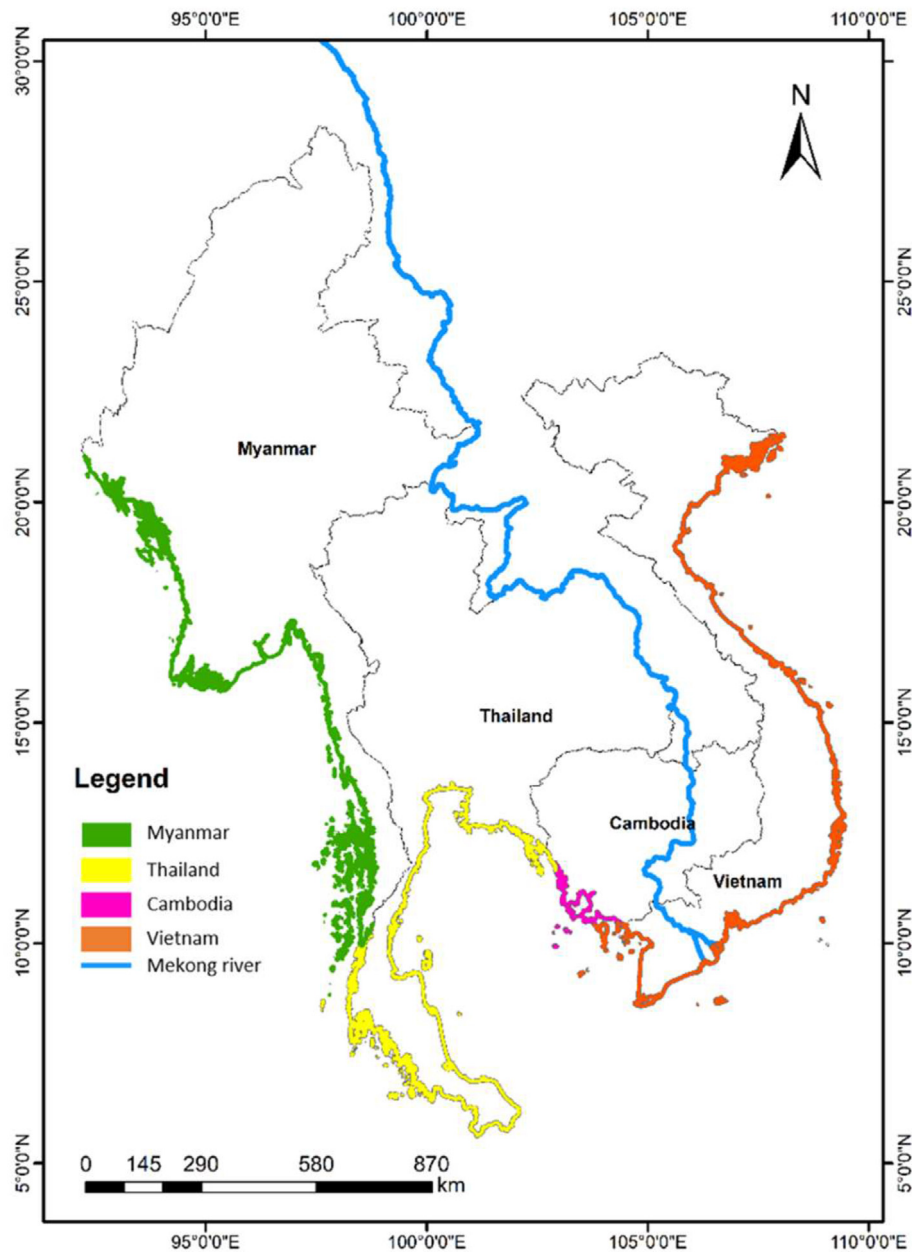| No.	Year	Landsat	Data Composite Period
1	1989	Landsat 5	1989-01-01 to 1989-12-31
2	1995	Landsat 5	1995-01-01 to 1995-12-31
3	2000	Landsat 5	2000-01-01 to 2000-12-31
4	2005	Landsat 5	2005-01-01 to 2005-12-31
5	2010	Landsat 5	2010-01-01 to 2010-12-31
6	2015	Landsat 8	2015-01-01 to 2015-12-31

Fig. 1. Geographical locations of the mangrove forests by countries in the Lower Mekong Region.

crafting and running of scripts for geospatial analysis and workflow processing (Google Earth Engine, 2021). The data acquisition phase encompassed the retrieval of Landsat 5 images from 1989 to 2010, and Landsat 8 imagery for the years 2015–2020. These acquired annual images were then subjected to further processing stages. Accordingly, a composite function was initiated utilizing GEE code to refine the images to median pixel values, while a cloud threshold of 95% was established to counteract the effects of cloud cover as recommended by Venkatappa et al. (2019). We used the cloud mask function to eliminate clouds and shadows. This cloud mask function is a tool developed by the Landsat Provisional Aquatic Reflectance and the United States Geological Survey (Landsat Provisional Aquatic Reflectance, 2021; USGS, 2021).

3.3. Application of the classification and Regression Tree algorithm

Previous studies have explored machine learning algorithms and classification techniques, such as unsupervised, supervised, hybrid, random forest, support vector machine, and object-oriented

classifications on the GEE (Johansen et al., 2015; Mondal et al., 2019). Based on these studies with high accuracy of the Classification and Regression Tree (CART) algorithm in mangrove area, the CART was also employed as the algorithm in our study. It is worth noting that CART functions as a rule-based classifier within a tree-structured decision space (Pallara, 1992).

Here, we classified the land into five distinct categories: mangroves, other vegetation, water bodies, urban areas, and barren land along the LMR coastlines based on the approach outlined by Giri et al. (2011). The category of other vegetation encompasses various land cover types such as grasslands, barren agricultural lands, and croplands. Water bodies comprise both marine and freshwater sources, including stagnant inland waters, while urban areas encapsulate human-made structures. In contrast, barren lands signify the eroded and degraded regions within the defined study area or buffer zone (Wang et al., 2018).

To facilitate a precise classification, we assigned multiple random training points to each land cover category (see Supplementary Information). A total of 250 training points were identified to maximize

accuracy for the mangrove forests and were thus chosen for delineating mangrove areas. Different numbers of training points were assigned to the remaining categories (refer to Table 2), summing up to 750 points used throughout the study. These included 200 points for other

vegetation and 100 each for water bodies, urban areas, and barren land. Supplementary Information elaborates further on the training points utilized.

For image training using the CART algorithm, the polygon geometry tools available in GEE were employed. The training points were distinctly color-coded: red for mangroves, green for other vegetation, blue for water bodies, yellow for urban areas, and grey for barren land, facilitating a vivid and clear classification process.

After the initial training phase on the GEE platform, the mangrove areas were delineated using the CART algorithm. Accordingly, we undertook stringent accuracy assessments and validation protocols, which are vital in steering informed decisions in mangrove conservation (Asner et al., 2010). This accuracy assessment was executed within the GEE platform, following the computation of the mangrove area. Furthermore, we instituted data validation steps before the estimation of carbon stocks and the evaluation of their fluctuations. A graphic overview of the complete methodology adopted in this study is illustrated in Fig. 2.

Table 2
Data point distribution for model training across land cover types.

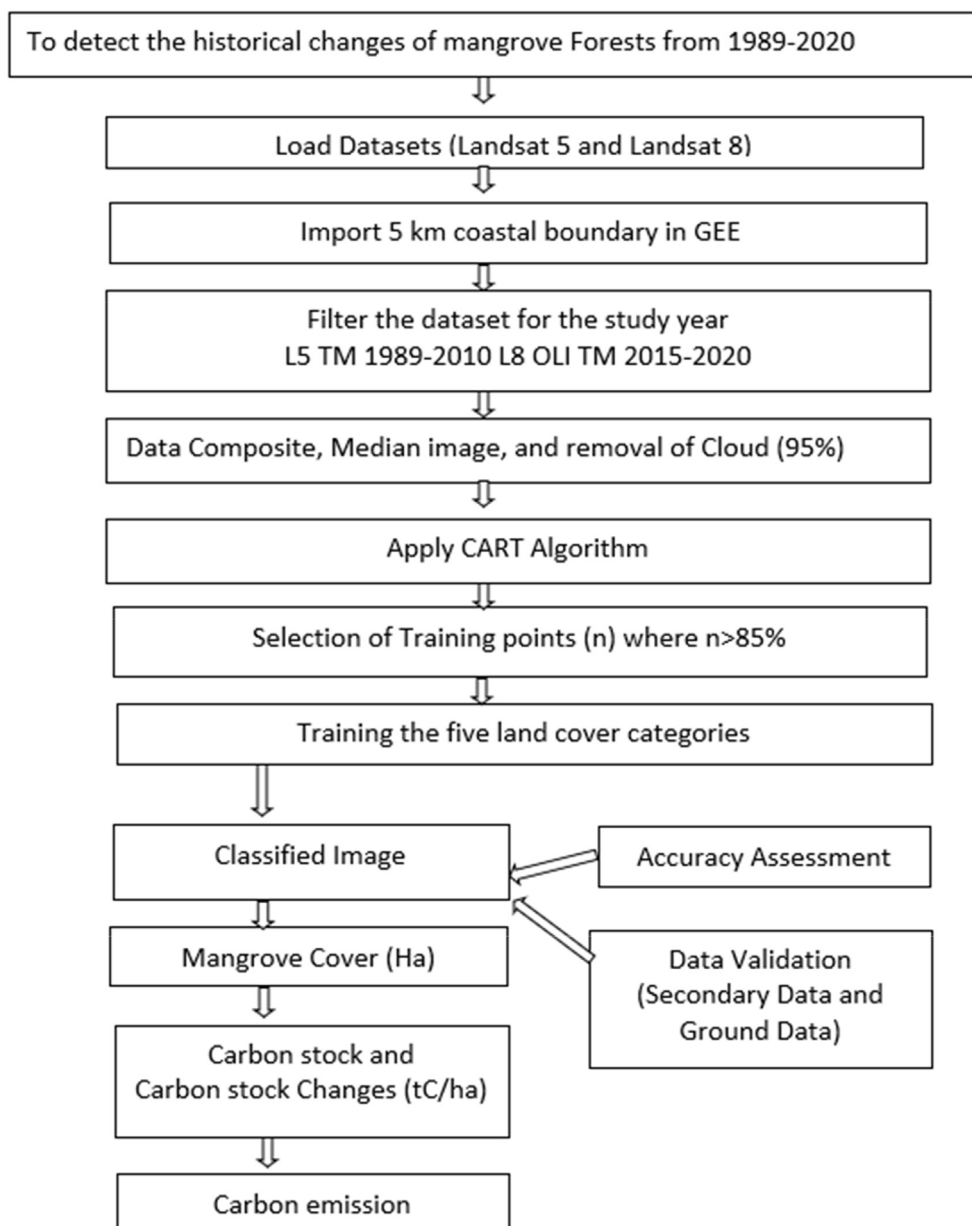| Points in GEE	Land cover type	Training points
	Mangrove	250
	Other vegetation	200
	Water	100
	Urban/Built Area	100
	Barren Land	100
Total Training points		750
		In total (750*7) = 5250

Fig. 2. Methodological framework depicting the flow from data acquisition to the estimates of carbon emissions.
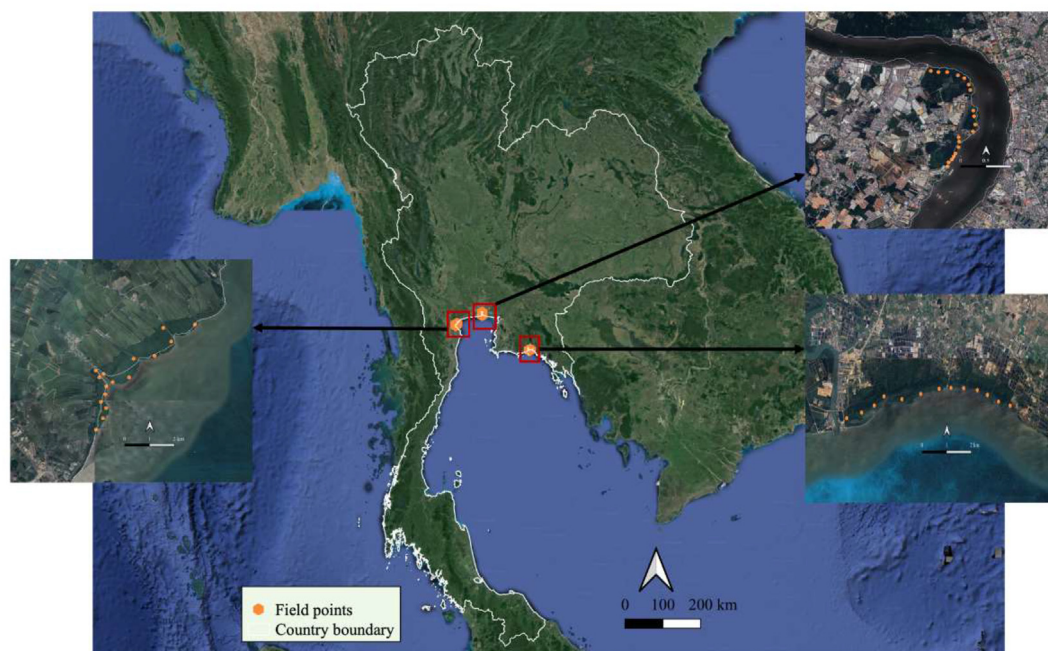
Fig. 3. Georeferenced locations of the field data collection sites in Thailand visualized in GEE.

Table 3
Average carbon stock values in five mangrove carbon pools.

Carbon pools	CS (MgC ha^{-1})	CS (MgCO$_2$)
AGB	185	678.37
BGB	78.63	288.32
Litter	9.64	35.34
Soil	447.00	1639.00
Deadwood	16.34	59.92
Total average	**736.61**	**2700.95**

3.4. Accuracy assessment and ground truthing

An accuracy assessment was accomplished by utilizing a confusion matrix on the GEE platform. The overall accuracy percentages calculated for the years 1989 through 2020 were 88%, 92%, 93%, 88%, 94%, 95%, and 95%, respectively. Kappa coefficients, derived from the confusion matrices for each year, yielded values of 0.84, 0.89, 0.90, 0.83, 0.92, 0.94, and 0.93. The CART algorithm thus exhibited an average accuracy of 92.1% for the LMR, with an average kappa coefficient of 0.89.

To ascertain the accuracy and diminish bias in our assessment, ground truthing complemented by secondary data was employed. Ground truthing involved collecting data through a Geographic Processing System (GPS) in Thailand at Samut Prakan, Samut Songkran, and Rayong during early January 2020. These locations were chosen for their varied geographical characteristics. Recorded GPS data were depicted in Fig. 3 and subsequently incorporated into ArcMap 10.3.1 to create a shapefile. This file was then used within GEE to corroborate the mangrove areas identified via remote sensing. Fig. 3 presents the overlay of reference points from Samut Songkran on a global dataset obtained from ArcGIS, validating the consistency of field data with the mangrove classifications on GEE imagery.

3.5. Calculation of carbon stocks and emissions in mangrove forests

To assess the carbon stocks and emissions from mangrove forests, we applied equation (1), derived from the sum of various carbon pools proportionate to mangrove area, following IPCC (2006) guidelines.

Carbon stock,

$$CS(t) = FArea(t) \times (CS_{AGB} + CS_{BGB} + CS_L + CS_D + CS_S) \quad (1)$$

In Eq. (1), the CS(t) represents the total carbon stock of the forest in tonnes of carbon per hectare (MgC ha^{-1}), FArea (t) denotes the area of the mangrove forest, CS_{AGB} represents carbon stored above ground, CS_{BGB} represents carbon stored below ground, CS_L represents the carbon stock of litter, CS_D represents the carbon stock of deadwood, and C_{SS} represents the carbon stock in the soil per hectare. Where

FArea(t) is Mangrove forest area at time t (in ha)

CS_{AGB} is Aboveground carbon stock (MgC ha^{-1})

CS_{BGB} is Belowground carbon stock (MgC ha^{-1})

CS_L is Carbon stock in the litter (MgC ha^{-1})

CS_D is Deadwood carbon stock (MgC ha^{-1})

CS_S is Soil carbon stock (MgC ha^{-1})

We derived carbon stock data from four pools as per Hutchison et al. (2014), while deadwood estimates were adopted from Suarez et al., 2019, following the approximation methods of Upakankaew and Shrestha (2018). These calculations yield a total carbon stock of 736.6 MgC ha^{-1}, as depicted in Table 3.

This carbon stock of 736.6 MgC ha^{-1} is well within the previous estimates at various countries around the world (Table 4). For instance, Dao et al. (2022) reported 489.5 MgC ha^{-1} for Vietnam's Mekong Delta mangroves and Dung et al. (2016) estimated between 573.5 and 1026.0 MgC ha^{-1}. Thailand's mangroves hold about 596.5 MgC ha^{-1} according to Chutamas and Chutamas (2019), while Cambodia's figures stand at 494.3 MgC ha^{-1} as per Sasaki et al. (2014). The Indo-Pacific mangroves, including the Sundarbans and Micronesia, show above and below-ground stocks of 1023 MgC ha^{-1} (Donato et al., 2011; Woltz et al., 2022). In West Central Africa, mangroves have a higher mean carbon stock at 799.0 MgC ha^{-1} with approximately 86% in the soil. The Asia-Pacific region reports even higher averages at 1094 MgC ha^{-1}. Nevertheless, Kauffman and Bhomia (2017) suggest a global average of 780 MgC ha^{-1} for mangroves.

Table 4
Mangrove forest cover in Myanmar, Thailand, Cambodia, and Vietnam (1989–2020).

Year	Myanmar (ha)	Thailand (ha)	Cambodia (ha)	Vietnam (ha)	Total Area (ha)
1989	784,685	339,613	83,754	365,608	1,573,660
1995	757,117	366,800	77,648	353,013	1,554,578
2000	488,970	322,427	55,123	277,448	1,143,968
2005	582,126	339,510	87,890	251,983	1,261,509
2010	690,712	475,515	81,266	357,794	1,605,287
2015	1,191,514	681,683	1,45,330	438,585	2,457,112
2020	1,000,080	601,642	117,664	345,078	2,064,464

To calculate changes in carbon stocks resulting from alterations in mangrove forest cover, we utilized the following equation:

$$CE(t) = [CS(t) - CS(t-1)] \times (44/12) \qquad (2)$$

Where.

CE(t) is the annual change of carbon stocks measured in terms of emissions if CS(t) > CS(t-1) or removals if otherwise (MgCO$_2$).

CS(t-1) represents the carbon stock in the previous year (also calculated using Eq. (1)). By subtracting the previous year's carbon stock from the current year's carbon stock.

The ratio 44/12 is the molecular weight of CO$_2$ over carbon.

4. Results

4.1. Trends of mangrove cover in the LMR between 1989 and 2020

In the Lower Mekong Region (LMR), Myanmar has the largest share of mangrove coverage, accounting for 48.4% of the total. Historical data indicates that Myanmar's mangrove cover was 784,685 ha in 1989, but it decreased to 757,117 ha by 1995 and continued to decline, reaching 488,970 ha by 2000, the period of most significant loss. A recovery was observed as forest cover increased to 582,126 ha in 2005 but a substantial rebound was observed with the mangrove cover expanding to 1,000,080 ha in 2020 (Fig. 4). The Ayeyarwady region, a key area for mangrove conservation in Myanmar, exhibited varying mangrove cover trends during the period studied.

Thailand had the second-largest mangrove area in the LMR, at 29.2% of the total. From 1989 to 2020, mangrove cover nearly doubled, growing from 339,613 ha to 601,642 ha. The lowest coverage was in 2000 at 322,427 ha, but an overall increase was seen, peaking at 681,683 ha in 2015, then slightly decreasing by 2020. Significant loss periods were between 1995-2000 and 2015–2020. Vietnam accounted for 16.71% of the LMR's mangroves, with a slight 5.6% decrease from 1989 to 2020, from 365,608 ha to 345,078 ha. The decline continued until 2005, hitting a low of 251,983 ha, then reversed, reaching 438,585 ha in 2015. Fig. 6 shows the reduction in mangrove forests in southern Vietnam, notably in Ben Tre and Than Phu, especially between 2005 and 2015. On the other hand, Cambodia had the smallest mangrove area in the LMR, 5.7% of the total. However, it saw a 40% increase in mangrove area from 1989 to 2020, from 83,754 ha to 117,664 ha. The area dropped to 55,123 ha in 2000 but increased until 2005, decreased until 2010, and peaked at 145,330 ha in 2015 before declining in 2020 (Fig. 5). Major reductions occurred from 1989 to 2000, 2005–2010, and 2015–2020.

By 2020, the mangrove cover in the LMR had increased by 31.2% from its 1989 extent, rising from 1,573,660 ha to 2,064,464 ha. The increase followed an initial decline, aligning with the forest transition theory, as indicated by the trends in Myanmar, Thailand, and Cambodia between 1989 and 2015. However, a decrease post-2015 is observable, as shown in Fig. 6. A closer look from 1989 reveals that mangrove cover in Myanmar, Thailand, and Cambodia generally trended upwards until 2020, unlike in Vietnam, where a reduction occurred. The timeframe from 1995 to 2000 experienced the sharpest decline, while the period from 2010 to 2015 witnessed the most considerable expansion.

With a mangrove forest cover of 1,573,712 ha in 1989, the LMR saw a marginal reduction to 1,554,578 ha by 1995. The downward trend continued in the following years, with a reversal seen leading to 2015. Vietnam and Myanmar were notably affected by mangrove deforestation within the LMR. Figs. 5 and 6 detail the changes in specific mangrove areas in Myanmar and Vietnam, respectively.

Employing the 30-m resolution satellite imagery to assess the mangrove extent, Giri et al. (2011) estimated the mangrove forest cover at 1,015,752 ha in the LMR in 2000. Their estimate is slightly lower than the estimate by our study, which was estimated 1,143,968 ha in 2000 (see Supplementary Information for details). Fig. 7 showcases this comparison: areas pinpointed in our analysis are marked in red, while the previously recorded data by Giri and colleagues appear in a darker tone. FAO's assessment for 2000 reported 844,161 ha of mangroves in the LMR (as per SI-II), a smaller figure than that given by Giri et al. (2011). Our analysis suggests a larger expanse of mangrove cover. Illustrated in Fig. 4, our study indicates additional inland mangrove areas not accounted for in earlier research. While Giri et al. focused largely on coastal and intertidal zones, our study encompasses inland, upland, and open ocean regions, which may explain the higher figure for mangrove coverage estimated in our assessment.

From 1989 to 2020, we found that the annual mangrove growth rates differed among the LMR countries. Myanmar had an average annual increase of 0.988%, Thailand experienced a significant 2.5%, Cambodia followed with 1.3%, and Vietnam displayed a slight rise at 0.18%. Notably, Thailand had the highest annual increase, ranging between 2.5% and 5.1%. Vietnam, on the other hand, had a consistently low growth rate over the three decades. These annual fluctuations are detailed in Table 5, and the underlying reasons for these variations in growth will be explored in subsequent analysis.

Carbon stock calculations took into account changes in mangrove area and carbon density. The area was determined using Google Earth Engine (GEE), and the average carbon density was taken as 736.6 MgC ha^{-1}, derived from various studies. The carbon stock calculations for Myanmar, Thailand, Cambodia, and Vietnam for the years 1989, 1995, 2000, 2005, 2010, 2015, and 2020 are presented in Table 6. For Myanmar, carbon stocks were estimated at 577.0 TgC, 557.0 TgC, 360.0 TgC, 428.0 TgC, 508.0 TgC, 877.0 TgC, and 736.0 TgC for the respective years. In Thailand, carbon stocks fluctuated between 250.0 TgC and 443.0 TgC, with per-hectare carbon densities ranging from 675.7 MgC to 757.0 MgC. Cambodia's carbon stocks were projected at 61.6 TgC, 57.2 TgC, 40.6 TgC, 64.7 TgC, 59.9 TgC, 107.0 TgC, and 86.7 TgC for the specified years. For Vietnam, estimated carbon stocks for these years were 269.0 TgC, 260.0 TgC, 204.0 TgC, 186.0 TgC, 264.0 TgC, 323.0 TgC, and 254.0 TgC.

4.2. Carbon emissions or removals due to mangrove forest cover changes in the LMR

The results of this study provide insights into the yearly carbon emissions from mangrove ecosystems across the LMR countries, with details shown in Table 7. Notably, negative figures in the table represent carbon sequestration by mangroves, indicating their role as carbon sinks rather than sources of emissions. In 2020, the mangrove forests in all four LMR countries collectively acted as carbon sinks.

From 2015 to 2020, every country in the LMR succeeded in achieving carbon sequestration within their mangrove forests. In the earlier period of 2010–2015, however, Myanmar and Thailand exhibited carbon emissions from mangrove ecosystems. It is essential to note that this study's national scale approach encountered challenges in pinpointing specific site-level variations. The period of 1995–2000, characterized by an increase in mangrove area, coincided with notable carbon sequestration. Mangroves are recognized for their high carbon storage capacity, with 1 ha of mangrove forest sequestering up to four times more carbon than many of the world's tropical forests, as reported by Donato et al. (2011). Among the countries analyzed, Myanmar's mangrove forests held
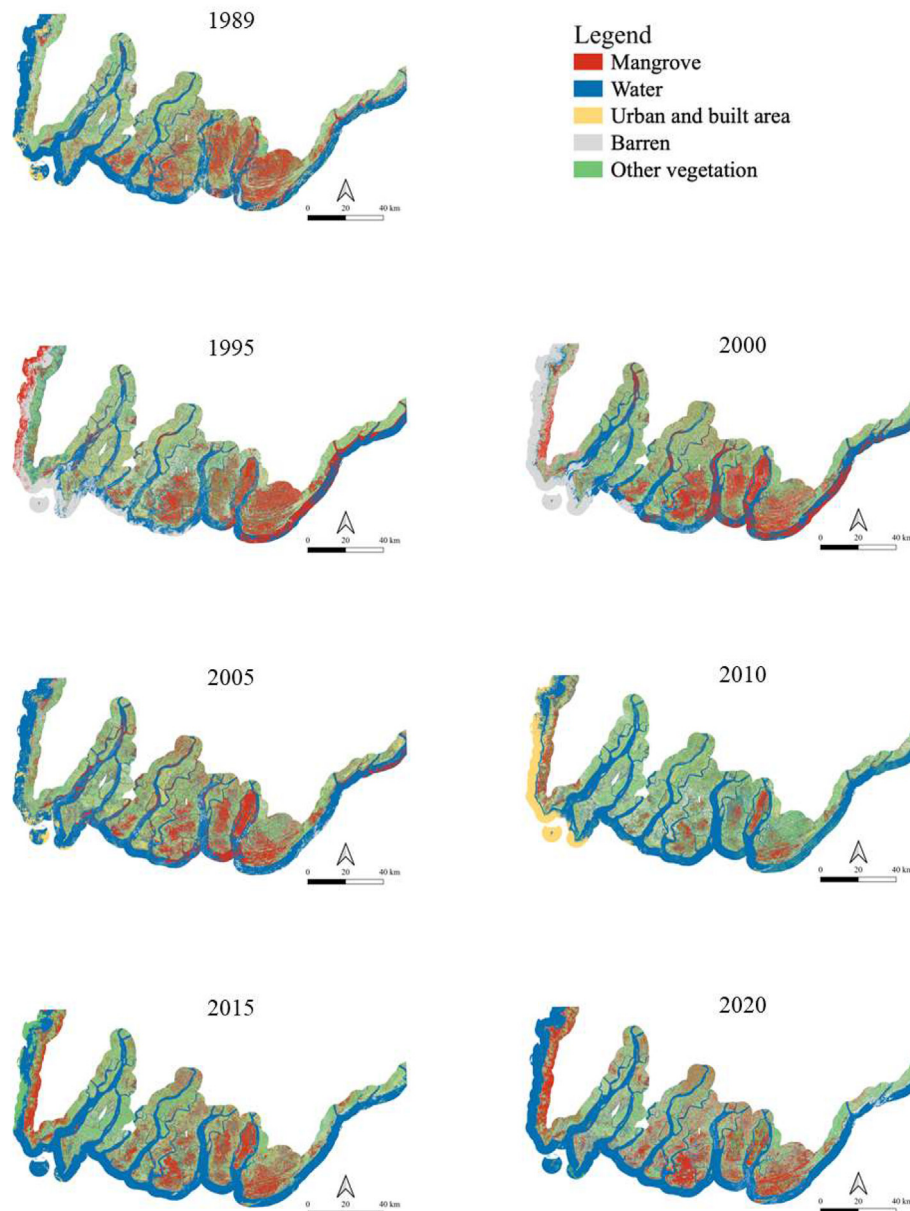
Fig. 4. Changes of mangrove forest area in Ayeyarwady, Myanmar between 1989 and 2020.

the highest potential for carbon stock. While the LMR's average carbon sequestration rate was lower than the global average, it still exceeded the rates found in many other regions and countries.

5. Discussions

5.1. GEE, accuracy, and mangroves

Using the Google Earth Engine (GEE), this study achieved a noteworthy average accuracy rate of 92.1% in the generated image of the LMR using the CART method, characterized by a respectable kappa coefficient average of 0.89. Several parallel studies using GEE for mangrove assessment have cited similar accuracy levels, substantiating the reliability of this tool in scientific endeavors. For example, the mangrove mapping in Brazil from 1985 to 2018 noted an accuracy of 87% (Diniz et al., 2019), while in Cambodia the vegetation type threshold values were delineated with an 85% accuracy rate (Venkatappa et al., 2019). Other studies in West Africa and Sierra Leone documented accuracies of 90% and 95% respectively (Mondal et al., 2017, 2019). Notably, a recent

study focusing on the northern coast of Vietnam depicted a remarkable accuracy of 92% (Vu et al., 2022). These efforts rely significantly on freely accessible data and potent algorithms bolstering effective supervision and delineation of forest cover transformations and Sustainable Development Goals indicators (Mondal et al., 2019; FAO, 2020).

Utilizing the CART algorithm in our study rendered a more precise output compared to secondary data available for the year 2000. Despite the high accuracy achieved, a few errors in area estimation during the GEE training phase were inevitable. These errors predominantly occurred in the classification of year-round and stationary water bodies, which were occasionally misconstrued as evergreen vegetation instead of mangroves. A minor decrement in overall accuracy was observed due to the visibility of other vegetation in shallow water areas. Nevertheless, these minor setbacks did not significantly affect the mangrove forest area estimation as an optimized number of training points were selected after numerous trial sessions, with 250 points proving most effective in achieving highest accuracy during training (SI-II). Accurate mangrove area estimation continues to be a complex endeavor due to intrinsic intricacies (Zhao & Qin, 2021). Our study, however, manages to fill the
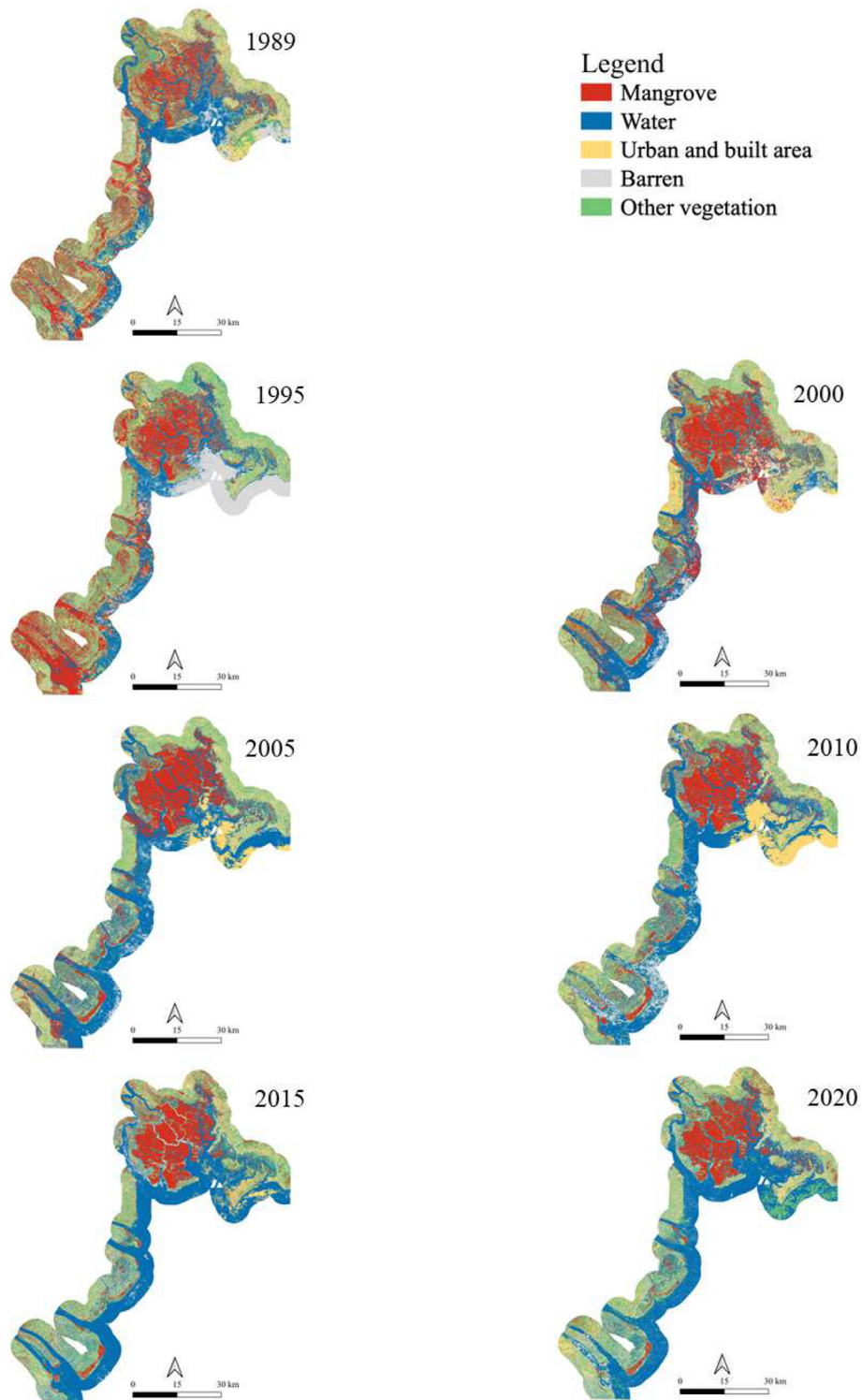
Fig. 5. Change of mangrove forest area in Southern Vietnam between 1989 and 2020.

data void concerning mangrove areas over several years, employing robust tools and apt methodologies, although further refinements are needed to curtail mapping errors (Powell et al., 2013).

Comparative studies, like that of Long and Giri (2011), leveraged Landsat imagery to assess mangrove cover in the Philippines, reporting an area of 256,185 ha in the year 2000, a figure notably higher than the 246,700 ha documented by the Food and Agriculture Organization (FAO) for the same year. The Department of Environment and Natural

Resources (DENR) stated an area close to the FAO's, at 247,362 ha. These variations primarily stem from the diverging methodologies and technologies employed in each study. The FAO assimilated both published and unpublished data, while the DENR utilized Landsat imagery, occasionally leading to broader misclassifications (Long & Giri, 2011). Hence, for more localized analysis or inter-regional comparisons, field research remains an indispensable approach for obtaining accurate data.
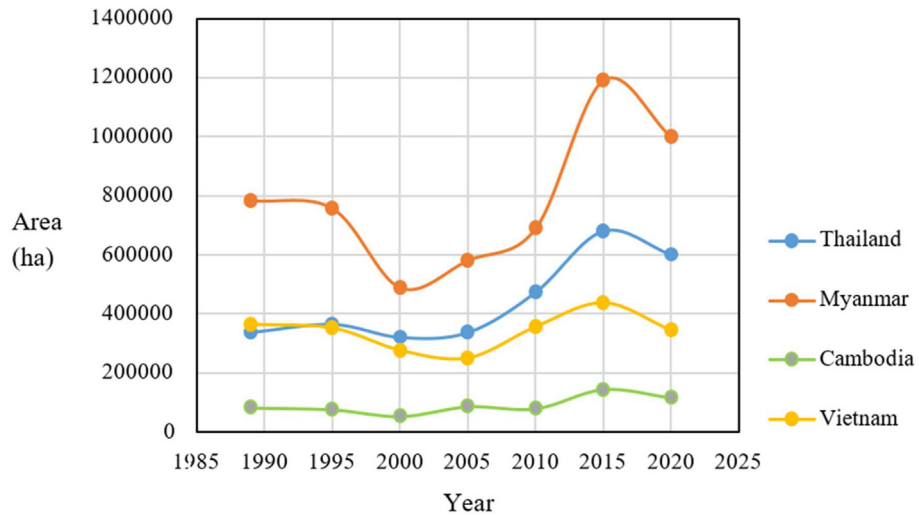
Fig. 6. Changes of mangrove forest area by countries in the LMR between 1989 and 2020.
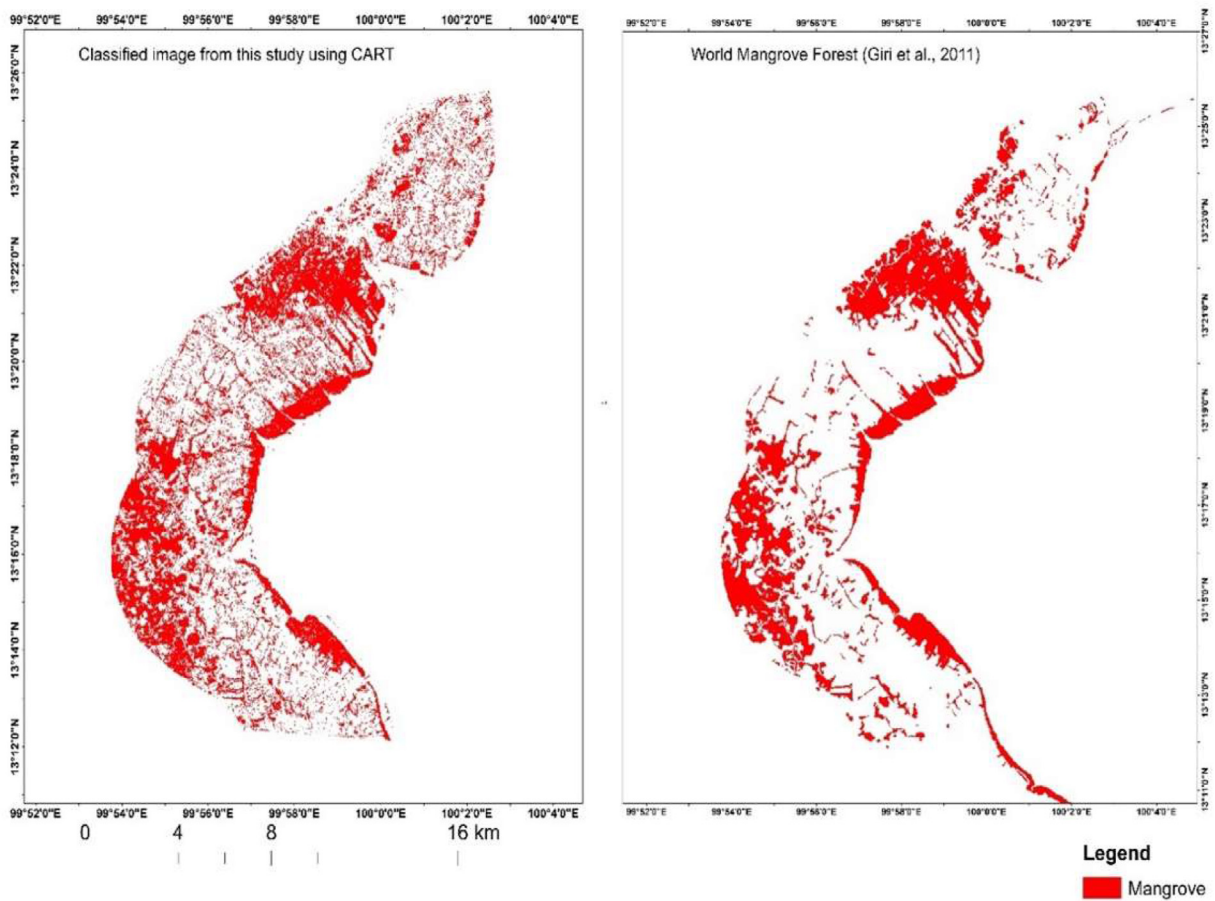

Fig. 7. Comparative analysis of CART-classified mangrove area (2000) and the data from Giri et al. (2011).

This study addresses the previous gap in lack of a standard method for mangrove estimation. The study will help governments in preparation of conservation plans and strategies for rehabilitation and taking proper actions for the sustainable management of mangroves in the LMR. To mitigate climate change, managers and policymakers need precise information on the status and spatial distribution of carbon sources and sinks. Without understanding the changes in mangrove forest cover, it would not be possible to provide effective policy interventions for reducing mangrove loss or reversing the trends.

5.2. Variations of carbon stocks in mangrove forests

The accuracy of mangrove cover estimations in our study is subject to potential errors from algorithm inaccuracies and classifier errors.

Table 5

Annual change rates of Mangrove Forests in LMR for every 5-year interval (in %).

Period	Myanmar	Thailand	Cambodia	Vietnam
1989–2020	0.88	2.5	1.3	0.18
1995–2020	1.28	2.6	2.0	−0.08
2000–2020	5.2	4.3	5.6	1.2
2005–2020	4.7	5.1	2.3	2.4
2010–2020	4.4	2.7	4.5	−0.35
2015–2020	−5.6	−2.3	−3.8	−4.2

Negative means loss of mangroves.

Table 6

Mangrove forest carbon stock (CS) by year in Myanmar, Thailand, Cambodia, and Vietnam (in TgC).

Year	Myanmar	Thailand	Cambodia	Vietnam
1989	577.9	250.2	61.7	269.3
1995	557.7	270.2	57.1	260
2000	360.2	237.5	40.6	204.4
2005	428.9	250	64.7	185.6
2010	508.8	350.3	59.9	263.6
2015	877.7	502.2	107	323.3
2020	736.6	443.2	86.7	254.2

Table 7

Annual carbon emissions and Sequestration from Mangrove Area Changes in Lower Mekong Countries (TgCO2).

Internals	Myanmar	Thailand	Cambodia	Vietnam
1989–1995	−14.9	14.04	−3.8	−6.2
1995–2000	−144.9	−23.4	−12.6	−40.3
2000–2005	50.8	9.9	17.4	−13.9
2005–2010	58.5	73.72	−3.9	57.8
2010–2015	270.8	111	34	43.5
2015–2020	−103.7	−43.2	−15.2	−50

Minus sign (−) refers to carbon sequestration or removals.

Complications such as the mixed pixel effect and tidal influence pose additional challenges to satellite-based mapping accuracy of the mangroves (Rocchini et al., 2013; Toosi et al., 2019; Baloloy et al., 2020; Gandhi & Jones, 2019). Furthermore, the transition in satellite data from Landsat 5 to Landsat 8 may have also influenced trend consistency, particularly during 2010–2015. On the other hands, carbon stocks of mangrove forests vary significantly from one country to another. Mangrove forests in the tropics hold an average of 1023 MgC ha^{-1}, about 49–98% of which are found in the soil organic carbon (Donato et al., 2011). Elsewhere in the tropics, carbon stocks in mangroves were reported at 212 ha-1 in Africa, 477.0 in Latin America, 400 MgC in Australia, 446 MgC in Malaysia (Alongi, 2002), 540 MgC in Micronesia (Ellison, 2000), 611 MgC in Indonesia (Simard et al., 2008), 486 MgC in Vietnam (Nguyen et al., 2018), and 448 MgC in Thailand (Rattanachot & Prawirum, 2020). To provide the most accurate representation of carbon stocks, this study integrated field data and remote sensing techniques to gauge mangrove carbon stocks, recognizing variations in carbon biomass due to geographical location, forest maturity, and species diversity. The average aboveground biomass (AGB) was 185 MgC ha^{-1}, with belowground biomass (BGB) at 78.63 MgC ha^{-1} (Hutchison et al., 2014). Carbon pool in the litters contributed 9.64 t ha^{-1}, and soil carbon was estimated at 447 MgC ha-1. This research applied both global and local valuation methods, amalgamating data from various studies for a comprehensive evaluation so as to address the variations of the data sources and availability,. A basic correlation analysis revealed a positive relationship between forest cover and carbon reduction, further supporting the significance of mangrove conservation in carbon sequestration. The coefficient of determination (R-squared) was found to be 0.62, indicating a strong association between the two variables.

Our study introduces a correlation analysis between forest cover and carbon reduction, highlighting the link between mangrove cover changes and carbon emissions. This analysis is crucial in understanding the environmental impact of mangrove deforestation and the significance of conservation efforts. Despite uncertainties in biomass estimation and carbon accounting, our approach underscores the importance of localized data and focused studies for accurate understanding of mangrove alterations and deforestation across diverse regions (Baker et al., 2004; Castillo et al., 2017; FAO, 2020; Sasaki et al., 2016).

6. Conclusion

In this study, we have assessed the dynamics of mangrove cover and associated carbon stocks in the Lower Mekong Region (LMR) across three decades. By employing the Classification and Regression Tree (CART) algorithm within the Google Earth Engine (GEE) framework and leveraging 30-m resolution Landsat Top of Atmosphere (TOA) imagery, we achieved an exceptional accuracy rate of 92.1% and a kappa coefficient of 0.89 in mapping mangroves. Our findings indicate significant mangrove losses in Myanmar, Thailand, Cambodia, and Vietnam, with the most notable depletions occurring during 1995–2000 and 2015–2020, despite a slight resurgence observed from 2010 to 2015. These patterns are reflective of a global trend, suggesting a shared trajectory of mangrove cover changes on a worldwide scale.

Crucially, our research illuminates the capacity for carbon capture by LMR mangroves, which exceeds that of many other forest types. In light of the commitments made by parties of the Paris Climate Agreement of the United Nations Convention on Climate Change, our insights are invaluable for securing financial support through the United Nations' REDD + program. Such funding would bolster mangrove conservation efforts by monetizing the reduction of carbon emissions or the enhancement of carbon stocks. Yet, there remains a critical need for in-depth, localized analysis to identify the distinct factors driving mangrove cover changes. To develop effective conservation strategies, understanding the nuances behind these drivers at the local level is essential. Therefore, we call for further research aimed at dissecting these factors with increased precision, enabling a comprehensive understanding of the elements that affect conservation policies. Through such focused investigations, we can enhance the strategic effectiveness of mangrove conservation and ensure the longevity and health of these vital ecosystems.

Declaration of competing interest

The authors declare that they have no known competing financial interests or personal relationships that could have appeared to influence the work reported in this paper.

Appendix A. Supplementary data

Supplementary data to this article can be found online at https://doi.org/10.1016/j.igd.2024.100140.

References

Alongi, D. M. (2002). Carbon sequestration in mangrove forests. *Journal of Environmental Management, 65*(2), 315–325.

Alongi, D. M. (2014). Carbon cycling and storage in mangrove forests. *Annual Review of Marine Science, 6*, 195–219. https://doi.org/10.1146/annurev-marine-010213-135020

Asner, G. P., Powell, G. V. N., Mascaro, J., Knapp, D. E., Clark, J. K., Jacobson, J., … Hughes, R. F. (2010). High-resolution forest carbon stocks and emissions in the Amazon. *Proceedings of the National Academy of Sciences, 107*, 16738–16742. https://doi.org/10.1073/PNAS.1004875107

Baker, T. R., Phillips, O. L., Malhi, Y., Almeida, S., Arroyo, L., Di Fiore, A., … Vásquez Martínez, R. (2004). Increasing biomass in Amazonian forest plots. *royalsocietypublishing.org, 359*, 353–365. https://doi.org/10.1098/rstb.2003.1422

Bacoloy, A. B., Blanco, A. C., Raymund Rhommel, R. R. C., & Nadaoka, K. (2020). Development and application of a new mangrove vegetation index (MVI) for rapid and accurate mangrove mapping. *ISPRS Journal of Photogrammetry and Remote Sensing, 166*, 95–117. https://doi.org/10.1016/J.ISPRSJPRS.2020.06.001

Bimrah, K., Dasgupta, R., Hashimoto, S., Saizen, I., & Dhyani, S. (2022). Ecosystem services of mangroves: A systematic review and synthesis of contemporary scientific literature. *Sustainability, 14*(19), Article 12051.

Castillo, J. A. A., Apan, A. A., Maraseni, T. N., & Salmo, S. G. (2017). Estimation and mapping of above-ground biomass of mangrove forests and their replacement land uses in the Philippines using Sentinel imagery. *ISPRS Journal of Photogrammetry and Remote Sensing, 134*, 70–85. https://doi.org/10.1016/J.ISPRSJPRS.2017.10.016

Chakravarty, S., Ghosh, S. K., Suresh, C. P., Dey, A. N., & Shukla, G. (2012). Deforestation: Causes, effects and control strategies. *Global perspectives on sustainable forest management, 1*, 1–26.

Chen, B., Xiao, X., Li, X., Pan, L., Doughty, R., Ma, J., … Giri, C. (2017). A mangrove forest map of China in 2015: Analysis of time series Landsat 7/8 and Sentinel-1A imagery in Google Earth Engine cloud computing platform. *ISPRS Journal of Photogrammetry and Remote Sensing, 131*, 104–120.

Chutamas, N., & Chutamas, W. (2019). Carbon stock and sequestration potential of mangrove forests in Thailand: A review. *International Journal of Climate Change Strategies and Management, 11*(6), 745–761.

Dao, T. H., Nguyen, T. D., Sasmito, S. D., Quang, V. H., Dung, T. M., Linh, T. V., & Van Kien, N. (2022). Carbon storage and sequestration in mangrove forests of the Mekong Delta, Vietnam. *Science of the Total Environment, 826*, Article 154053.

De Graaf, G. J., & Xuan, T. T. (1998). Extensive shrimp farming, mangrove clearance and marine fisheries in the southern provinces of Vietnam. *Mangroves and Salt Marshes, 23*(2), 159–166. https://doi.org/10.1023/A:1009975210487, 1998.

Diniz, C., Cortinhas, L., Nerino, G., Rodrigues, J., & Sensing, L. S.-R. (2019). Undefined Brazilian mangrove status: Three decades of satellite data analysis. mdpi.com. Available at: https://www.mdpi.com/439806. (Accessed 3 September 2021).

Donato, D. C., Kauffman, J. B., Murdiyarso, D., Kurnianto, S., Stidham, M., & Kanninen, M. (2011). Mangroves among the most carbon-rich forests in the tropics. *Nature Geoscience, 45*(4), 293–297. https://doi.org/10.1038/ngeo1123, 2011.

Dung, L. V., Tue, N. T., Nhuan, M. T., & Omori, K. (2016). Carbon storage in a restored mangrove forest in can gio mangrove forest park, Mekong delta, Vietnam. *Forest Ecology and Management, 380*, 31–40, 2016.

Ellison, J. C. (2000). Mangrove restoration: Do we know enough? *Restoration Ecology, 8*(3), 219–229.

FAO. (2007). *The world's mangroves 1980-2005* (Rome).

FAO. (2020). *Global forest Resources assessment 2020: Main report*. https://doi.org/10.4060/ca9825en. Rome.

FAO. (2020). *The state of the world's forests 2020*. FAO and UNEP. https://doi.org/10.4060/CA8642EN

FAO. (2023). *The world's mangroves 2000–2020*. https://doi.org/10.4060/cc7044en. Rome.

Gandhi, S., & Jones, T. G. (2019). Identifying mangrove deforestation hotspots in south Asia, Southeast Asia and asia-pacific. *Remote Sensing, 11*, 728. https://doi.org/10.3390/RS11060728, 2019, Vol. 11, Page 728.

Giri, C., Ochieng, E., Tieszen, L. L., Zhu, Z., Singh, A., Loveland, T., … Duke, N. (2011). Status and distribution of mangrove forests of the world using earth observation satellite data. *Global Ecology and Biogeography, 20*, 154–159. https://doi.org/10.1111/J.1466-8238.2010.00584.X

Google Earth Engine. Available at: https://earthengine.google.com/. (Accessed 3 September 2021).

Hamilton, S. E., & Casey, D. (2016). Creation of a high spatio-temporal resolution global database of continuous mangrove forest cover for the 21st century (CGMFC-21). *Global Ecology and Biogeography, 25*, 729–738. https://doi.org/10.1111/geb.12449

Hansen, M. C., Potapov, P. V., Moore, R., Hancher, M., Turubanova, S. A., Tyukavina, A., Thau, D., Stehman, S. V., Goetz, S. J., Loveland, T. R., Kommareddy, A., Egorov, A., Chini, L., Justice, C. O., & Townshend, J. R. G. (2013). High-resolution global maps of 21st-century forest cover change. *Science, 342*(6160), 850–853. https://doi.org/10.1126/science.1244693

Hutchison, J., Manica, A., Swetnam, R., Balmford, A., & Spalding, M. (2014). Predicting global patterns in mangrove forest biomass. *Conserv. Lett., 7*, 233–240. https://doi.org/10.1111/CONL.12060

Ibe, C. E., Ijeh, J. C., & Uhegbu, C. H. (2022). Mapping coastal land cover change using time series Landsat data and Google earth engine: A case study of the Niger delta, Nigeria. *Journal of Remote Sensing*, 1–20.

IPCC guidelines for national greenhouse gas inventories | Hydrotheek. Available at: https://library.wur.nl/WebQuery/hydrotheek/1885455. (Accessed 3 September 2021).

Jia, M., Wang, Z., Mao, D., Ren, C., Song, K., Zhao, C., Wang, C., Xiao, X., & Wang, Y. (2023). Mapping global distribution of mangrove forests at 10-m resolution. *Science Bulletin*. https://doi.org/10.1016/j.scib.2023.05.004

Jia, M., Wang, Z., Mao, D., Ren, C., Wang, C., & Wang, Y. (2021). Rapid, robust, and automated mapping of tidal flats in China using time series Sentinel-2 images and Google Earth Engine. *Remote Sensing of Environment, 255*, Article 112285.

Johansen, K., Phinn, S., & Taylor, M. (2015). Mapping woody vegetation clearing in queensland, Australia from Landsat imagery using the Google earth engine.

Remote Sens. Appl. Soc. Environ., 1, 36–49. https://doi.org/10.1016/J.RSASE.2015.06.002

Kanniah, K. D., Sheikhi, A., Cracknell, A. P., Goh, H. C., Tan, K. P., Ho, C. S., & Rasli, F. N. (2015). Satellite images for monitoring mangrove cover changes in a fast growing economic region in southern Peninsular Malaysia. *Remote Sensing, 7*, 14360–14385.

Kauffman, J. B., & Bhomia, R. K. (2017). Ecosystem carbon stocks of mangroves across broad environmental gradients in West-Central Africa: Global and regional comparisons. *PLoS One, 12*, Article e0187749. https://doi.org/10.1371/JOURNAL.PONE.0187749

Landsat Collections in Earth Engine and Earth Engine Data Catalog. Available at: https://developers.google.com/earth-engine/datasets/catalog/landsat. (Accessed 29 September 2021).

Landsat Provisional Aquatic Reflectance. Available at: https://www.usgs.gov/core-science-systems/nli/landsat/landsat-provisional-aquatic-reflectance. (Accessed 3 September 2021).

Le Billon, P. (2000). The political ecology of transition in Cambodia 1989-1999: War, peace and forest exploitation. *Development and Change, 31*, 785–805. https://doi.org/10.1111/1467-7660.00177

Long, J. B., & Giri, C. (2011). Mapping the Philippines' mangrove forests using Landsat imagery. *Sensors, 11*, 2972–2981. https://doi.org/10.3390/S110302972

Lovelock, C. E., Barbier, E., & Duarte, C. M. (2022). Tackling the mangrove restoration challenge. *PLoS Biology, 20*(10), Article e3001836. https://doi.org/10.1371/journal.pbio.3001836

Malik, A., Mertz, O., & Fensholt, R. (2017). Mangrove forest decline: Consequences for livelihoods and environment in South Sulawesi. *Regional Environmental Change, 17*, 157–169.

Mondal, P., Liu, X., Fatoyinbo, T. E., & Lagomasino, D. (2019). Evaluating combinations of sentinel-2 data and machine-learning algorithms for mangrove mapping in West Africa. *Remote Sensing, 11*, 2928. https://doi.org/10.3390/RS11242928

Mondal, P., Trzaska, S., & de Sherbinin, A. (2017). Landsat-derived estimates of mangrove extents in the Sierra Leone coastal landscape complex during 1990–2016. *Sensors 2018, 18*, 12. https://doi.org/10.3390/S18010012. Page 12 18.

Nguyen, T. T. V., Tran, T. T. V., Nguyen, V. T., & Tran, H. D. (2018). Carbon stocks and sequestration rates of mangrove forests in the Red River Delta, Vietnam. *Wetlands Ecology and Management, 26*(3), 497–509.

Pallara, A. (1992). Binary decision trees approach to classification. *Statistics and Applications, 4*, 255.

Powell, T. L., Galbraith, D. R., Christoffersen, B. O., Harper, A., Imbuzeiro, H. M. A., Rowland, L., … Moorcroft, P. R. (2013). Confronting model predictions of carbon fluxes with measurements of Amazon forests subjected to experimental drought. *New Phytologist, 200*, 350–365. https://doi.org/10.1111/NPH.12390

Rahman, M. R., & Deddy, M. (2021). Utilizing Google earth engine and multi-temporal Landsat data for mapping and monitoring mangrove forests in the Sundarbans reserved forest, Bangladesh. *Journal of Environmental Management, 293*, Article 112847.

Rattanachot, Y., & Prawirum, C. (2020). Aboveground and belowground carbon stocks in different mangrove zones in Ranong, Thailand. *International Journal of Environment and Sustainable Development, 11*(10), 1–5.

Rocchini, D., Foody, G. M., Nagendra, H., Ricotta, C., Anand, M., He, K. S., … Neteler, M. (2013). Uncertainty in ecosystem mapping by remote sensing. *Computational Geosciences, 50*, 128–135. https://doi.org/10.1016/J.CAGEO.2012.05.022

Sasaki, N., Chheng, K., Mizoue, N., Abe, I., & Lowe, A. J. (2016). Forest reference emission level and carbon sequestration in Cambodia. *Glob. Ecol. Conserv., 7*, 82–96. https://doi.org/10.1016/J.GECCO.2016.05.004

Sasaki, N., Okubo, S., & Takeuchi, K. (2014). Carbon storage in mangrove forests of Cambodia. *Carbon Management, 5*(2), 213–222.

Sasmito, S. D., Basyuni, M., Kridalaksana, A., Saragi-Sasmito, M. F., Lovelock, C. E., & Murdiyarso, D. (2023). Challenges and opportunities for achieving Sustainable Development Goals through restoration of Indonesia's mangroves. *Nature Ecology & Evolution, 7*(1), 62–70.

Sathe, S. S., Lavate, R. A., Bhosale, L. J., & Vasantraodada, P. D. (2013). Mangrove as source of energy for Rural development with special reference to Ratnagiri and Sindhudarg district (MS) India. *Bioscience Discovery, 4*(2), 198–201.

Saxena, A., & Jain, S. (2017). Mangroves: Afforestation and sanctuaries. *Voyager, VIII*(2), 195–204. Dec 2017.

Simard, M., Fatoyinbo, T., Smettem, K. R., & Lovelock, C. E. (2008). Mangrove canopy height and biomass from TanDEM-X interferometry in Sarawak, Malaysia. *Remote Sensing of Environment, 112*(5), 2198–2210.

Song, X. P., Hansen, M. C., Stehman, S. V., Potapov, P. V., Tyukavina, A., Vermote, E. F., & Townshend, J. R. (2018). Global land change from 1982 to 2016. *Nature, 560*(7720), 639–643.

Suarez, D. R., Rozendaal, D. M. A., De Sy, V., Phillips, O. L., Alvarez-Dávila, E., Anderson-Teixeira, K., , … Martius, C., et al. (2019). Estimating aboveground net biomass change for tropical and subtropical forests: Refinement of IPCC default rates using forest plot data. *Global Change Biology, 25*, 3609–3624. https://doi.org/10.1111/GCB.14767

Thomas, N., Lucas, R., Bunting, P., Hardy, A., Rosenqvist, A., & Simard, M. (2017). Distribution and drivers of global mangrove forest change, 1996–2010. *PLoS One, 12*, Article e0179302. https://doi.org/10.1371/JOURNAL.PONE.0179302

Toosi, N. B., Soffianian, A. R., Fakheran, S., Pourmanafi, S., Ginzler, C., & Waser, L. T. (2019). Comparing different classification algorithms for monitoring mangrove cover changes in southern Iran. *Glob. Ecol. Conserv., 19*, Article e00662. https://doi.org/10.1016/J.GECCO.2019.E00662

United Nations Convention to Combat Desertification. (2014). Land degradation neutrality: Resilience at local, national and regional levels. Available at: https://catalogue.unccd.int/858_V2_UNCCD_BRO_.pdf. (Accessed 11 December 2023).

United Nations Convention to Combat Desertification. (2022). Global land outlook 2. Available at: https://www.unccd.int/sites/default/files/2022-04/UNCCD_GLO2_low-res_2.pdf. (Accessed 11 December 2023).

Upakankaew, K., Ninsawat, S., Virdis, S. G. P., & Sasaki, N. (2022). Discrimination of mangrove stages using multitemporal sentinel-1 C-band backscatter and sentinel-2 data – a case study in Samut songkhram province, Thailand. *Forests, 13*, 1433.

Upakankaew, K., & Shrestha, R. (2018). Detection of mangrove forest changes and assessment of carbon stock and economics values in samuth songkram, Thailand using remote sensing and. Scgi.Gistda.or.Th. Available at: http://scgi.gistda.or.th/wp-content/uploads/2018/02/SCGI2018-019.pdf.

USGS Landsat science products. Available at: https://www.usgs.gov/core-science-systems/nli/landsat/landsat-science-products?qt-science_support_page_related_con=2#qt-science_support_page_related_con. (Accessed 3 September 2021).

Venkatappa, M., Sasaki, N., Shrestha, R. P., Tripathi, N. K., & Ma, H.-O. (2019). Determination of vegetation thresholds for assessing land use and land use changes in Cambodia using the Google earth engine cloud-computing platform. *Remote Sensing, 11*, 1514. https://doi.org/10.3390/RS11131514, 2019, Vol. 11, Page 1514.

Vu, T. T. P., Pham, T. D., Saintilan, N., Skidmore, A., Luu, H. V., Vu, Q. H., … Matsushita, B. (2022). Mapping multi-decadal mangrove extent in the northern coast of Vietnam using Landsat time-series data on Google earth engine platform. *Remote Sensing, 14*(18), 4664.

Wang, Q., Lu, H., Chen, J., Hong, H., Liu, J., Li, J., & Yan, C. (2018). Spatial distribution of glomalin-related soil protein and its relationship with sediment carbon sequestration across a mangrove forest. *The Science of the Total Environment, 613–614*, 548–556. https://doi.org/10.1016/J.SCITOTENV.2017.09.140

Wang, C., Wang, F., Wang, Q., Yang, D., Li, L., & Zhang, X. (2013). Preparing for Myanmar's environment-friendly reform. *Environmental Science & Policy, 25*, 229–233. https://doi.org/10.1016/j.envsci.2012.08.014

Woltz, V. L., Peneva-Reed, E. I., Zhu, Z., Bullock, E. L., MacKenzie, R. A., Apwong, M., Krauss, K. W., & Gesch, D. B. A. (2022). Comprehensive assessment of mangrove species and carbon stock on Pohnpei, Micronesia. *PLoS One, 17*(7), Article e0271589. https://doi.org/10.1371/journal.pone.0271589

Xie, Z., Phinn, S. R., Game, E. T., Pannell, D. J., Hobbs, R. J., Briggs, P. R., & McDonald-Madden, E. (2019). Using Landsat observations (1988–2017) and Google Earth Engine to detect vegetation cover changes in rangelands - a first step towards identifying degraded lands for conservation. *Remote Sensing of Environment, 232*, Article 111317.

Xiong, J., Thenkabail, P. S., Tilton, J. C., Gumma, M. K., Teluguntla, P., Oliphant, A., … Gorelick, N. (2017). Nominal 30-m cropland extent map of continental Africa by integrating pixel-based and object-based algorithms using sentinel-2 and landsat-8 data on Google earth engine. *Remote Sensing, 9*, 1065. https://doi.org/10.3390/RS9101065, 2017, Vol. 9, Page 1065.

Zhao, C., & Qin, C.-Z. (2021). The key reason of false positive misclassification for accurate large-area mangrove classifications. *Remote Sensing, 13*, 2909. https://doi.org/10.3390/RS13152909